 doi:10.20944/preprints202012.0207.v1

Article

The impact of ambient atmospheric mineral-dust particles on the calcification of lungs

Mariola Jabłońska [1], Janusz Janeczek [1*] and Beata Smieja-Król [1]

1 Institute of Earth Sciences, University of Silesia; mariola.jablonska@us.edu.pl (M.J.); beata.smieja-krol@us.edu.pl (B.S-K.)

* Correspondence: janusz.janeczek@us.edu.pl; Tel.: +48 323689261 (J.J.)

Abstract: For the first time, it is shown that inhaled ambient air-dust particles settled in the human lower respiratory tract induce lung calcification. Chemical- and mineral compositions of pulmonary calcium precipitates in the lung right lower-lobe (RLL) tissues of 12 individuals who lived in Upper Silesia Conurbation in Poland and who had died from causes not related to lung disorder were determined by transmission- and scanning electron microscopy. Whereas calcium salts in lungs are usually reported as phosphates, calcium salts precipitated in RLL are almost exclusively carbonates, i.e. Mg-calcite and calcite. These constitute 37% of 1652 mineral particles examined. Mg-calcite predominates in the submicron size range with the $MgCO_3$ content up to 50 mol%. Magnesium plays a significant role in the lung mineralization, a fact so far overlooked. The calcium phosphate (hydroxyapatite) content in RLL is negligible. The predominance of carbonates is explained by increased CO_2 fugacity in RLL. Carbonates enveloped inhaled mineral-dust particles, including uranium-bearing oxides, quartz, aluminosilicates, and metal sulfides. Three possible pathways for the carbonates precipitation on the dust particles are postulated: (1) precipitation of amorphous calcium carbonate (ACC) followed by its transformation to calcite; (2) precipitation of Mg-ACC followed by its transformation to Mg-calcite; (3) precipitation of Mg-free ACC causing a localized relative enrichment in Mg ions and subsequent heterogeneous nucleation and crystal growth of Mg-calcite. The actual number of inhaled dust particles may be significantly greater than observed because of the masking effect of the carbonate coatings. There is no simple correlation between smoking habit and lung calcification.

Keywords: air pollution, lung mineralization, magnesian calcite, calcite, amorphous calcium carbonate

1. Introduction

Pulmonary calcification involves the precipitation of calcium salts in lung tissues. Numerous causes of pathogenic calcification are grouped into metastatic, dystrophic, and idiopathic causes [1-3]. Metastatic calcification, both benign and malignant, refers to calcium deposition in normal tissues caused by high levels of serum calcium and phosphate, and dystrophic calcification to the deposition of calcium salts in previously injured cells and tissues. Dystrophic calcification includes calcification triggered by asbestosis, silicosis, coal-miner's pneumoconiosis, and other occupational diseases caused by inhaled mineral dust [1,2]. Metastatic calcification is composed chiefly of either amorphous or microcrystalline whitlockite, $(Ca,Mg)_3PO_4$, with subordinate pyrophosphate [4]. According to Farver [3], calcium is usually in the form of calcium phosphate. Dystrophic calcification is a localized process leading to deposition of crystalline hydroxyapatite (HAP) [1]. The rare idiopathic lung disorder known as pulmonary alveolar microlithiasis causes the deposition of micronodules composed of either calcium phosphate [5-6] or calcium carbonates ([2].

Lung calcification is routinely diagnosed by X-ray chest radiography or computed tomography. These techniques do not enable the mineral species building of the calcium "lesions" to be determined. Hence, usually no attempts are made to distinguish between the various possible

 doi:10.20944/preprints202012.0207.v1

calcium salts deposited. Instead, morphological aspects of calcification are important in etiology and treatment.

While the adverse effect of large numbers of mineral particles on human cardiopulmonary health is well known [7-15], there have been no attempts to relate lung calcification to inhaled ambient atmospheric dust particles. Moreover, Ca-bearing particles encountered in lung tissues are assumed to be indicators for tobacco smoke [16]. In this paper, by examining the mineral composition of lung lower lobe (RLL) tissues of 12 individuals from the Upper Silesia Conurbation (USC), Poland, we show that endogenous particles of Ca- and (Ca, Mg)-carbonates in lung tissues may originate in response to the settlement of inhaled atmospheric dust particles.

2. Mineral inventory of inhaled dust particles

Mineral assemblages found in lungs are endogenous, i.e., formed biogenically *in situ*, and exogenous (inhaled). The former includes Ca-carbonates, Ca-phosphates, and, rarely, Ca-oxalates. Quantities of mineral particles inhaled by people not occupationally exposed to dust can be quite high. Approximately 10^{11} ultrafine (<0.1μm in diameter) dust particles may be deposited daily in the respiratory tract of a person living in the Los Angeles area [17]. The life-time accumulation of mineral dust particles in the lungs of non-occupationally exposed North American urban dweller is on average 0.5×10^9 particles per gram of dry lung [18]. The geometric mean of total particle contents in the lungs of the Mexico City inhabitants is 2.055×10^6 particles/g dry lung and approximately ten time less in those of residents in Vancouver, Canada [16].

Brauer et al. [16] examined the parenchymal particle contents of autopsy lungs from never-smoking female residents of Mexico City and Vancouver. From their observations, 96% of the retained particles were < 2.5μm in aerodynamic diameter, including aggregated ultrafine particles. Brauer et al. [16] concluded that individuals residing for a long time (> 60 years) in an area of high ambient particle concentrations retain much greater numbers of those particles compared to long-term residents of an area of low ambient pollution levels.

The mineral composition of dust inhaled due to occupational exposures is well established (e.g., [19-20]). However, less is known of the mineral composition of dust particles deposited in the lungs of those who were not occupationally exposed to dust. The pioneering studies in this respect were of Churg and Wiggs [21] and Churg et al. [22] in Vancouver, Paoletti et al. [23] in the Rome area, and Stettler et al. [18] in Cincinnati, Ohio. The majority of particles observed in these studies were rock-forming minerals, including free silica (dominant quartz), aluminosilicates (feldspars), and layered silicates (clays, kaolinite, micas, talc).

Microanalysis of lung autopsy tissues of individuals exposed to the catastrophic London smog episode in December 1952 revealed aggregates of ultrafine (≤ 0.1 μm) carbonaceous material associated with fine (≤ 1.0 μm) heavy-metal-bearing particles [24]. Domingo-Neumann et al. [25] analyzed the ashed lung samples of 30 subjects from Fresno, California, and found that mineral composition of dust particles (quartz, plagioclase, K-feldspars, biotite) to be similar to that of particulate matter with an aerodynamic diameter < 10μm (PM_{10}) sampled during field agricultural operations in that region. A recent SEM study of 33 lung tissue samples from individuals exposed to desert dust and other sources of inhaled particulate matter revealed 51 distinct phases among 13000 particles examined; the most common phases were of silica (a collective term for both crystalline- and amorphous silicon dioxide), feldspars, apatite, titanium oxides and iron oxides [26].

As expected, all of the sources quoted above show that the mineral inventory of exogenous particles settled in human lungs reflects that of dust particles in ambient air. Not surprisingly, the most abundant particles are of natural aluminum silicates (feldspars and mica) and silica. These are typical constituents of continental crust and, as such, they are the predominating dust particles in non-industrial regions. The relative abundance of titanium oxides (Cincinnati) and talc (Cincinnati, Rome, Vancouver) resulted from their wide use. All of the observed minerals were emitted either from natural sources or were released due to anthropogenic activities.

3. Site characterization

Preprints (www.preprints.org) | NOT PEER-REVIEWED | Posted: 8 December 2020 doi:10.20944/preprints202012.0207.v1

The Upper Silesian Conurbation (USC) is located in the center of the Silesian province (voivodship) in southern Poland. The USC consists of 14 adjacent cities with a total population of 1.85 million [27]. Together with an additional 15 directly bordering communities, the USC forms one of the most urbanized- and industrialized regions of Europe with ca. 2.5 million people. The USC is the most densely populated region of Poland (on average 887 persons/km^2 and 3785 persons/km^2 in one of the cities). Despite significant improvement in air quality since the beginning of political- and economic transformations in Poland in 1989, air pollution in the USC still causes serious environmental- and health problems. Residential coal-burning, the major emission source of air pollutants in the region, accounted for 66% of PM_{10}, 76% of $PM_{2.5}$, and 94% of benzo[a]pyrene in 2018 [28]. Industrial sources (electricity- and heat generating coal-fired plants, metal manufacturers including steel mills, zinc and copper smelters and refineries, coking and chemical plants, coal mines) account for 14% and 15% of PM_{10} and $PM_{2.5}$, respectively. Unlike in other European metropolitan areas, the vehicular transport contribution to air pollution is relatively low (5%PM_{10} and 4%$PM_{2.5}$) despite the large number of motor vehicles and extensive network of high-traffic roads.

Between 2010-2018, the $PM_{2.5}$ mean annual concentrations in all cities of the USC exceeded the annual limit value of 25 μg/m^3 [27]. The seasonal peak in airborne particle concentrations occurs during the heating season (usually late October to late April); it is caused by coal- and biomass-burning for domestic heating. The $PM_{2.5}$ concentration in winter is twice that in summer. For instance, the average $PM_{2.5}$ concentration during the winter of 2018 in Katowice, the capital of the USC, was 47 μg/m^3 compared to 22 μg/m^3 in summer [27]. In winter, the air quality is classified as unhealthy for sensitive groups, and unhealthy or very unhealthy for more than 60% of the time. During unfavorable weather conditions (stagnant dry air, temperature inversion), the air quality may reach the hazardous category. The seasonality of peak ambient air pollution is reflected in the seasonal exacerbation of respiratory diseases [29]. The daily average mortality due to cardio-respiratory disorders in the USC is significantly higher in winter than in summer and it correlates well with high daily $PM_{2.5}$ concentrations [30]. A relationship between an increased morbidity to lung cancer in males and elevated concentrations of PM_{10} in ambient air has been observed in Upper Silesia [31]. Some 20% of those with diagnosed lung cancer in Upper Silesia were non-smokers (never smoked) and had never been exposed occupationally to carcinogenic substances. Thus, they may have been environmentally exposed to respirable dust and other carcinogenic agents.

Most of the constituents of ambient atmospheric dust in the USC are anthropogenic, including rock-forming minerals that may have been released during mineral processing or construction [32]. Major airborne dust phases include: quartz (>20 vol.%), soot (<10 vol. % in summer and up to 90 vol. % in winter), fly-ash (20 vol. % throughout the year), gypsum (20 vol. % in winter), and Fe-oxides (hematite, magnetite, wüstite). In addition to the major constituents, over 30 minor- or accessory mineral phases have been identified in atmospheric dust samples in the USC [32-34].

A comparison of the exogenous-particle inventory observed in samples of the lung right lower lobe (RLL) of 12 individuals who lived in the USC (Table 1) with that of atmospheric particulate matter reveals a close similarity with the notable exceptions of soot and graphite [33]. Though soot and graphite commonly occur in the USC atmospheric particulate matter, they have not been observed in RLL. Chemical compositions and particle morphologies encountered in atmospheric dust and in lungs are identical. However, the assemblages differ in relative mineral proportions. Calcite and its Mg-rich variety are predominant in lung samples whereas carbonates, with dolomite dominating, are subordinate components (<8 vol.%) of the airborne particulate matter, and they have distinctly different morphologies [34].

Table 1. Mineral composition, number (n), content (vol.%), and sizes of particles observed in RLL tissues of lungs of 12 individuals in the USC. Compiled and modified from data in [33].

Mineral phase	n	Content (vol. %)		Size (μm)	
		mean	range	mean*	range
Carbonates	612	32	5.5-65	1.42(06)	0.22-5.05
Al-silicates[1]	243	19	12-34	2.10(12)	0.26-5.01

Preprints (www.preprints.org) | NOT PEER-REVIEWED | Posted: 8 December 2020 doi:10.20944/preprints202012.0207.v1

Silica[2]	149	10	3-17	1.90(12)	0.35-4.65
Fe-oxides[3]	199	12	5-30	1.67(11)	0.31-4.98
Halides[4]	112	7	2-9	1.69(15)	0.54-5.04
Iron	35	2	1-4	1.74(36)	0.42-4.93
Sulfides[5]	53	3	1-5	1.36(22)	0.34-4.08
Metals[6]	49	3	0.4-7	1.72(29)	0.22-5.02
Spinels[7]	38	3	1-4	1.83(31)	0.17-5.08
Alloys[8]	39	2	1-4	1.58(30)	0.25-4.33
Oxides[9]	53	2	0-7	1.13(17)	0.17-4.46
Gypsum	26	2	2-5	2.11(32)	0.68-4.76
Barite	32	2	1-5	1.25(22)	0.42-3.60
Ca-phosphate	9	1	1-3	2.70(70)	0.68-4.76
REE-phosphates	3	0.5	0.3-0.9	1.47(26)	0.97-2.08

Mineral phases observed in lung tissues of all 12 subjects are in bold;* numbers in brackets refer to standard deviation; [1]include spherical amorphous (vitrous) aluminosilicates (fly-ash) (ca. 20 vol.%), feldspars, mullite, amphiboles, clay minerals (illite, talc); [2]quartz, tridimite, and amorphous silica (ca.11 %); [3]hematite, magnetite, wüstite, goethite, ferrihydrite; [4]halite, sylvite; [5]galena, sphalerite, and Fe-sulfides; [6]Au, Sn, Pb, Ti; [7]magnesioferrite, franklinite, herzinite, jacobsite; [8]Cu-Ni-Zn alloys and steel; [9]oxides other than spinels and Fe-oxides: brookite (TiO_2), Sn, Zr, Zn–oxides;

4. Materials and Methods

Autopsy samples of lung tissues from 12 USC residents (4 females and 8 males), 18 to 89 years old at a time of death not related to lung diseases, were provided by the DiagnoMed company and a clinical hospital in Zabrze together with information on age, sex, smoking habit and medical record of each subject. Ten individuals were never occupationally exposed to dust. Two individuals were retired coal miners aged 81 and 87. Seven individuals, including the former coal miners, were life-long smokers. None of the individuals had a record of lung disorders. All samples were from the RLL and consisted of non-tumoral subpleural tissues. The size of each sample was 2x2x0.5 cm.

The samples, after drying at 37°C, were examined by transmission electron microscopy (TEM) and scanning electron microscopy (SEM). Samples for TEM were prepared by gently crushing fragments of lung tissues in a mortar and placing them on a standard copper mesh grid. Observations and analyses were performed using JEOL JEM-2000FX (accelerating voltage 200 keV) and JEOL JEM-3010 (accelerating voltage 300 keV) microscopes. Phase identification was done by combining energy dispersive X-ray spectrometry (EDX) and selected area electron diffraction (SAED) data. Secondary electron (SE) and back-scattered electron (BSE) images of uncoated samples were acquired using an environmental analytical scanning electron microscope Phillips 30XL equipped with an EDAX EDS Sapphire system operated at 15 keV accelerating voltage. Pressure in the sample chamber was 0.3 Torr. Carbon coated samples were observed using a high-vacuum scanning electron Inspect F microscope with field emission operated at accelerating voltages of 15 and 20 keV.

The size of individual mineral particles was measured in two dimensions using calibrated SEM and TEM images and Visio Drawing 2000 (Microsoft) software. The equivalent diameter of particles was determined as a root-mean-square size, $\{a^2 + b^2\}^{1/2}$, where a and b are the two greatest orthogonal distances between points on the particle perimeter. Based on those measurements the volume concentration (V_c) was calculated from the formula:

$$Vc = \frac{m}{n} \times 100\% \pm u_\alpha \sqrt{\frac{\frac{m}{n}(1-\frac{m}{n})}{n}} \times 100\%,$$

where m is the sum of equivalent diameters of all particles of a given mineral species, n is the sum of equivalent diameters of all mineral particles in the sample, u_α is the critical value of the distribution function for a given confidence level.

Mineral-saturation indices were computed using PHREEQC software [35] for both human blood plasma and simulated lung fluid (Gamble's solution).

Preprints (www.preprints.org) | NOT PEER-REVIEWED | Posted: 8 December 2020 doi:10.20944/preprints202012.0207.v1

5. Results and discussion

Carbonates constitute 37% of 1652 mineral particles examined in the investigated samples. Carbonates contents vary from 5.48 vol.% in the tissues of an 18 year-old smoking female to 64.62 vol.% in the tissues of an 82-year old non-smoking female. The mean value is 31.94 ± 0.29 vol.% (Table 2). The highest concentration of carbonates among males (43.59 vol.%) was observed in the tissues of 87-year old life-long smoker. The highest number of carbonate particles (102) associated with the highest number of mineral particles (289) was observed in the tissues of a 54-old male smoker. The quantities of carbonates in RLL of non-smoking females is higher than that those in both smoking- and non-smoking males of the same or similar age (Table 2). Among males, the amounts of carbonates tend to be higher in the tissues of non-smoking individuals. A plausible explanation for this observation is that smoking causes a decrease in the pH of lung fluids, inhibiting precipitation of carbonates. This accords with the measured elevated concentrations of Ca in the RLL of non-smoking individuals (3000-8000 ppm) compared to smokers (<1500 ppm; [33]).

Table 2. Contents of carbonate particles (CP) related to the total number of mineral particles (TP) and sizes (μm) of CP in RLL tissues of 12 individuals from the USC.

	Females				Males							
Age	18s	54ns	65ns	82ns	30s	46s	53ns	54s	74s	81sm	82ns	87sm
CP/TP	6/83	49/1177	66/1122	77/108	49/211	29/158	24/113	102/289	28/85	95/201	26/68	46/107
vol. %	5.48	36.05	41.57	64.62	21.06	18.65	21.09	28.50	29.20	38.29	40.09	43.59
diameter range	0.68-2.48	0.37-4.46	0.23-3.51	0.38-5.05	0.30-4.45	0.22-4.98	0.44-3.14	0.23-4.43	0.39-4.25	0.22-3.58	0.52-3.97	0.56-3.90

s – smoker; n – nonsmoker; m – coal miner

Carbonates occur as clusters of polycrystalline aggregates ranging from 0.5-7 μm in diameter or as single crystals ranging from 0.2-5 μm in length (Figure 1). The largest (7 μm) particles are agglomerates of smaller subgrains. The mean equivalent diameter of the carbonate particles is 1.42 μm ± 0.06 (n = 612; variation coefficient = 57%). Single particles have smooth surfaces and sharp edges (Figure 1).

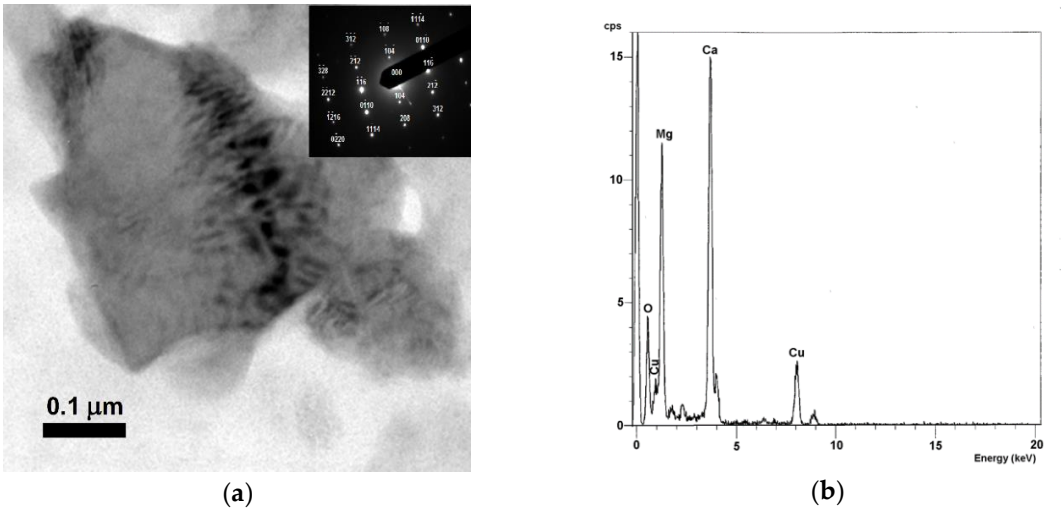

(**a**) (**b**)

Figure 1. (**a**) TEM image, SAED pattern, and (**b**) EDS spectrum of Mg-calcite crystal from RLL tissue of 30-year old male smoker.

Unlike the ubiquitous carbonates, only 9 calcium phosphate (hydroxyapatite, HAP) particles were found in the tissues of 5 male individuals, four of whom were life-long smokers. The maximum number of the observed HAP particles in a single sample was 3 in tissues of two individuals 30 and 54 years old. Samples of two other individuals contained single particles. The equivalent diameter of the HAP particles ranged from 2.02 to 3.77 μm. Volumetrically, HAP constitutes only 1.25-2.76 % of

Preprints (www.preprints.org) | NOT PEER-REVIEWED | Posted: 8 December 2020 doi:10.20944/preprints202012.0207.v1

all mineral particles and HAP/carbonates values range from 0.02-0.06. The lesser occurrence of HAP relative to that of carbonates is further reflected in the lack of correlation between Ca and P concentrations in RLL [33].

Four carbonate species, namely, amorphous calcium carbonate (ACC), calcite ($CaCO_3$), Mg-calcite ($Ca_{1-x}Mg_xCO_3$) and dolomite ($CaMg(CO_3)_2$), were identified by SAED and EDS. Electron diffraction patterns of the Mg-calcite particles match the standard (amcsd_0001327) of biogenic magnesium calcite. The hexagonal unit cell parameters calculated from $d_{3\bar{2}\bar{4}}$ (1.515 Å) and $d_{\bar{1}38}$ (1.283 Å) are: a = 4.966 Å, c = 16.714 Å, V = 412.19 Å^3. These are smaller than the unit cell parameters calculated for the amcsd_0001327 standard (a = 4.972 Å, c = 16.927 Å, V = 418.45 Å^3).

The number of dolomite particles in the RLL tissues ranged from 2-6 per sample, i.e., <10% of all carbonate particles. They were distinguished from Mg-calcite by SAED patterns. Airborne dolomite, a common constituent of dust particles in the USC, originates from the quarrying of dolomite deposits and from the natural weathering of dolomite outcrops in the region [34]. Thus, the dolomite particles are considered to be exogenous in the lung tissues.

Out of 612 observed carbonate particles, 64 (10.5%) are submicron (<1 μm) in size. Mg-calcite is the most abundant (50 particles, 78%) submicron carbonate (Figure 1) with Mg-free calcite constituting the remainder (14 particles, 22%). Together, calcite and Mg-calcite constitute 26% of all submicron particles in the RLL tissues examined (Figure 2).

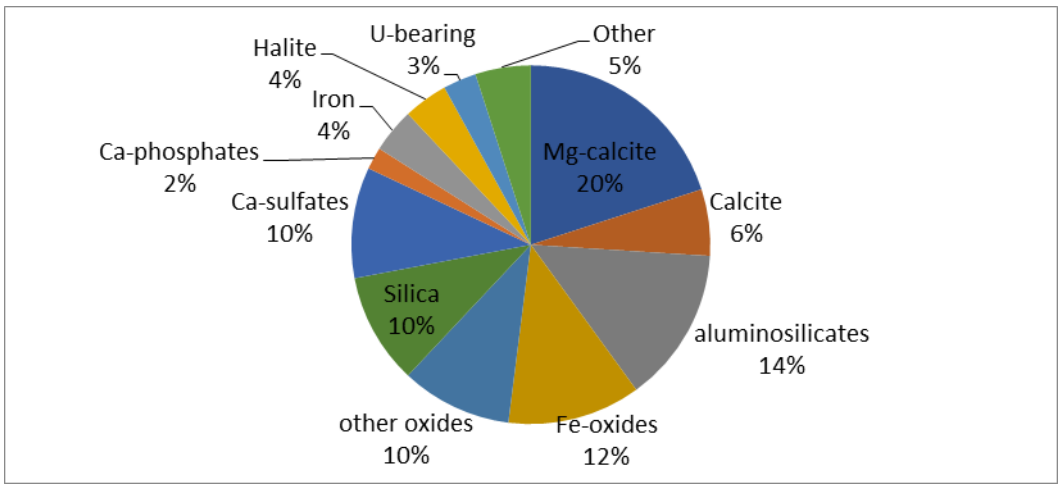

Figure 2. Mineral composition of submicron particles in RLL tissues of 12 individuals from the USC.

Values of $K_\alpha Mg/K_\alpha Ca$ peaks intensity ranging from 0.33-1.13 (mean 0.75) in the EDS spectra of 48 Mg-calcite particles suggests a wide range of Mg contents in the Mg-calcite. Due to technical problems (rough particle surfaces, small size), obtaining reliable quantitative data on chemical composition of the Mg-calcite proved difficult. Standardless semi-quantitative EDS microanalysis of Ca and Mg in 5 carbonate particles gave $MgCO_3$ mole percentages of 29, 31, 47, 52 and 53. These values are typical for very high magnesian calcite (30-45 mol% $MgCO_3$) and disordered dolomite, i.e., proto-dolomite with 46-50 mol% $MgCO_3$ [36]. From the Mg/Ca value in a simulated lung fluid (SLF) composition provided by Taunton et al. [37], which is identical to the Mg/Ca in human blood plasma [38], the $MgCO_3$ content in Mg-calcite precipitated from either SLF or blood plasma is expected to be 37.5 mol%.

Preprints (www.preprints.org) | NOT PEER-REVIEWED | Posted: 8 December 2020 doi:10.20944/preprints202012.0207.v1

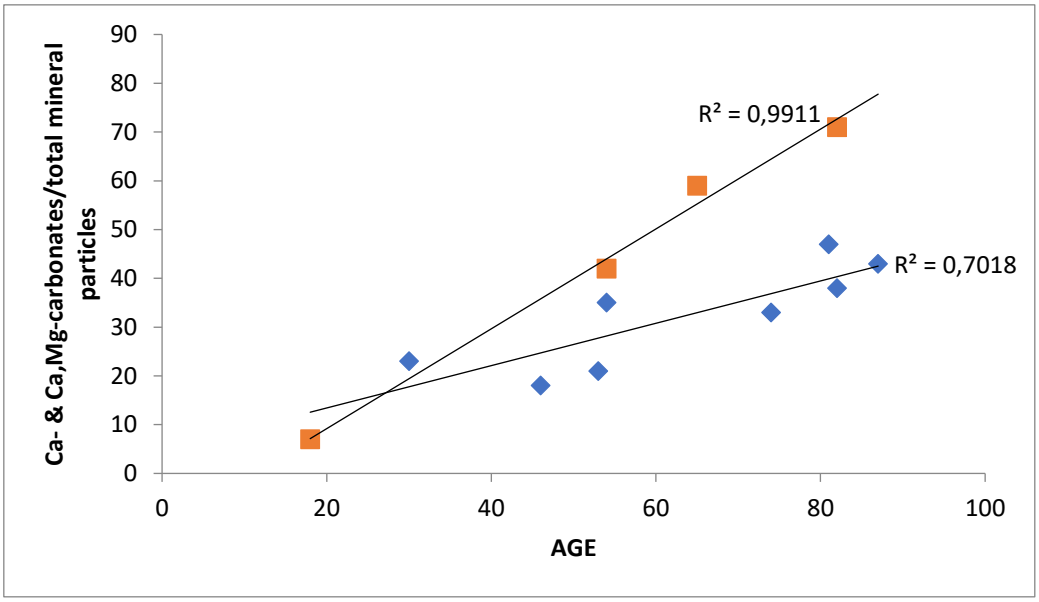

Fig. 3. Ratio of carbonates to the total amount of mineral particles in RLL tissues of 12 individuals from the USC vs. their age (squares – female; diamonds – male).

There is a positive correlation between the amounts of carbonates related to the total of mineral particles and the age of individuals (Figure 3). This correlation is particularly strong in samples from females, despite a limited dataset. In the RLL of the elderly, carbonates occur as clusters of numerous particles covering large portions of the observed tissues (Figure 4). The increase in the quantity of carbonates with age relative to the amount of exogenous mineral particles suggests that precipitation of the carbonates may have been induced by inhaled dust particles. This suggestion is confirmed by the dust particles embedded in carbonates.

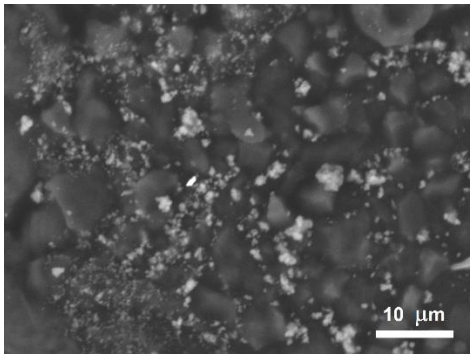

Fig. 4. SEM image of Mg-calcite and calcite incrustations (bright grains) on RLL tissues of an 81-year old former miner and life-long smoker.

Calcite often envelops particles of Fe-, Zn- and Pb-sulfides [33]. During this study, submicron particles of quartz and aluminosilicates enclosed in crystalline Mg-calcite were observed in RLL tissues (Figure 5). These observations show that the exogenous mineral particles served as nuclei for the precipitation of endogenous carbonates.

Preprints (www.preprints.org) | NOT PEER-REVIEWED | Posted: 8 December 2020 doi:10.20944/preprints202012.0207.v1

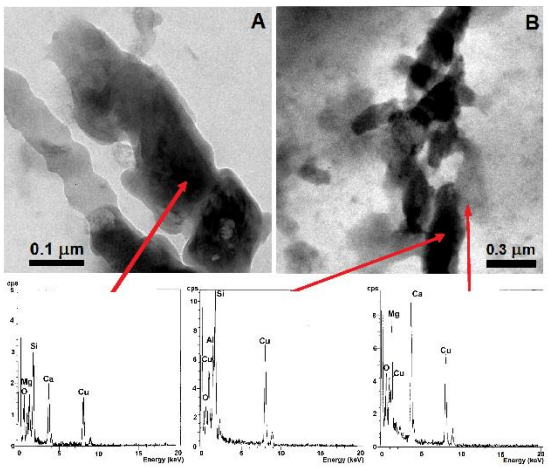

Figure 5. TEM images and related EDS spectra of Mg-calcite-coated: (A) silica and (B) aluminosilicate particles deposited in RLL of individuals from the USC.

Of particular interest is the observation of uranium oxide (perhaps, uraninite) and Fe-rich particles coated by ACC (Figure 6), suggested by the diffuse halos in the SAED patterns. Uranium-bearing particles, often associated with soot, have been observed in airborne mineral dust samples collected at several sites in the USC (Figure 6A). Their occurrence resembles uraninite nanocrystals encapsulated in carbonaceous matter in suspended particulates released from coal-fired power plants in Detroit [39]. Thus, it is no surprise to find uranium-bearing particles in the lungs of people living in places affected by coal combustion. The strong Fe peak in the EDS spectrum of a U-bearing particle in lung tissue may reflect Fe-bearing phase/phases either associated with the inhaled U-bearing particle (Figure 6A) or may have originated in the process of phagocytosis [40].

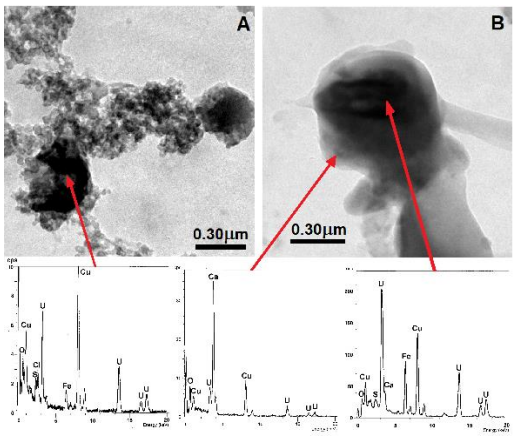

Fig. 6. TEM images and related EDS spectra of (A) uranium-oxide particles and Fe-phase attached to the airborne soot aggregate collected in the USC and (B) uranium-oxide particle and Fe-phase both coated by ACC in RLL tissue of 62-year old male non-smoker.

The ACC coating on the uranium-bearing particle (Figure 6B) may have been a precursor of calcite according to current models for biogenic calcite formation [41-44]. The biogenic formation of calcite is a two-stage process that involves initial precipitation of thermodynamically unstable ACC, which spontaneously and rapidly crystallizes to calcite either directly or through a nanocrystalline vaterite intermediate. The transformation of vaterite to calcite is a sluggish process, ten times slower than the transition from ACC to vaterite. However, in the presence of organic matter and/or Mg, calcite is stabilized over vaterite [42]. No evidence for vaterite was observed during this study.

The predominance of Mg-calcite among submicron carbonates suggests that their amorphous precursor was also enriched in Mg. Laboratory experiments show a 1:1 dependence on the Mg/Ca

Preprints (www.preprints.org) | NOT PEER-REVIEWED | Posted: 8 December 2020 doi:10.20944/preprints202012.0207.v1

ratio in solution and carbonate precipitated from that solution [43], [45]. However, the EDS spectra of the ACC coating of U-bearing particles (Figure 6) do not show X-ray peaks from Mg.

We hypothesize that there are three possible carbonate-precipitation pathways in lungs triggered by exogenous dust particles: (1) Precipitation of ACC on dust particles followed by its transformation to calcite; (2) precipitation of Mg-ACC followed by its transformation to Mg-calcite; (3) precipitation of Mg-free ACC followed by Mg-calcite heterogeneous nucleation and crystal growth. The last pathway requires a localized increase in Mg/Ca in the lung fluid due to calcium consumption by the ACC. The relative enrichment in Mg may enable the direct precipitation of Mg-calcite on the Mg-free ACC. Perhaps, localized specific biochemical conditions regulate the selection of these pathways in the process of phagocytosis.

While calcium salts precipitated in lungs are most frequently identified as phosphates (hydroxylapatite and/or whitlockite), calcium carbonate is also reported in numerous cases. Fine acicular crystals of calcite have been found in lung tissue of individuals affected by berylliosis, sarcoidosis and tuberculosis [46]. Calcium carbonate has been found in the so-called pulmonary "blue bodies" – roughly spherical laminated structures in the cytoplasm of alveolar macrophages [47]. Under specific chemical conditions, other types of calcium salts may form in human lungs. Calcium monohydrate oxalate (mineral whevellite, $CaC_2O_2 \cdot H_2O$) may occur in lung tissue affected by infection with *Aspergillus* species [46]. Thus, the type of calcium salt precipitated in lungs depends on the local biochemical conditions.

In response to the intrusion of a foreign body into the alveolar cells of lungs, a substantial increase in intracellular Ca^{+2} released from both mitochondria and the endoplasmic reticulum occurs [2, 48-49]. The influx of Ca^{+2} is sufficient to enable precipitation of either apatite or calcite. Thus, carbonate- and phosphorous ions are competing for Ca in the lung fluids.

Experiments using simulated lung fluids (SLF) at pH 7.4 and 37°C show that HAP is a preferred precipitate because the initial SLF is supersaturated with respect to HAP (saturation index SI = log(ion activity product/solubility product) = 6.9 [37]. Taunton et al. [37] confirmed their calculations with observations by SEM/EDS on large (30×10 μm) calcium phosphates particles comprising the predominant phase in calcified pleural plaques in the lungs of 85-year old male welder and smoker. However, the concentration of HCO_3^- (0.0321 mol/L) in the SLF used by Taunton et al. [37] is an order of magnitude greater than that of HPO_4^{2-} (0.00104 mol/L).

Table 3. Saturation index (SI), ion activity product (IAP), and solubility product (Ksp) for carbonates and hydroxyapatite (HAP) computed from compositions of simulated lung fluid (Gamble's solution) and blood plasma.

Phase	Gamble's solution			Blood plasma		
	SI	log IAP	log Ksp	SI	log IAP	log Ksp
calcite	1.12	-7.44	-8.56	0.70	-7.86	-8.56
dolomite	2.10	-15.26	-17.36	1.43	-15.93	-17.36
HAP	7.77	3.32	-4.45	6.52	2.08	-4.45

The saturation index calculated for calcite from compositions of SLF (Gamble's solution) and human blood plasma [38] during our study is 1.12 and 0.70, respectively (Table 3). Interestingly, both fluids are even more supersaturated (SI = 1.43 and 2.10, respectively) with respect to dolomite which can be considered as a compositional analogue for Mg-calcite. While saturation index values for both carbonates are lower than for HAP (SI = 7.77 in Gamble's solution and 6.52 in blood plasma), they are positive making precipitation of carbonates possible. Therefore, based solely on the chemical compositions of human blood plasma and SLFs, both precipitation pathways, i.e., phosphatic and carbonatitic, are possible. Whether calcium is bound to phosphate or to carbonate precipitates apparently depends on the CO_2 fugacity (P_{CO2}). According to Chan et al. [2], the high ventilation (movement of air into and out of the lungs) to perfusion (flow of blood in the pulmonary capillaries) ratio of 3.3 resulting in relatively low P_{CO2} (ca 30 mm Hg) and a blood pH of 7.51 predispose the

Preprints (www.preprints.org) | NOT PEER-REVIEWED | Posted: 8 December 2020 doi:10.20944/preprints202012.0207.v1

apexes of lungs to the precipitation of calcium phosphate. In the lower lobes, the pH is more acidic (7.39) due to higher P_{CO2} (ca 44 mm Hg) and the ventilation to perfusion ratio is much lower (0.63; [50]). The increase in P_{CO2} in lower lobes favors precipitation of carbonates because most of the CO_2 reacts with water in the presence of the catalyst carbonic anhydrase in erythrocytes [51] to produce weak carbonic acid that dissociates into the bicarbonate ion:

$$CO_2 + H_2O \leftrightarrow H_2CO_3 \leftrightarrow HCO_3^- + H^+$$

Some 60% of the CO_2 in blood is transported as bicarbonate (HCO_3^-) favoring crystallization of carbonates according to the reaction:

$$HCO_3^- + Ca^{2+} \leftrightarrow CaCO_3\downarrow + H^+.$$

It has been shown experimentally that the HAP solubility increases significantly with an increase in P_{CO2} and that a small amount of calcite is precipitated at pH ca 7.4 and P_{CO2} = 0.01-1.0 bar [52].

Apparently, the lower lobe biochemical conditions are suitable for the precipitation and crystallization of both Mg-calcite and calcite in response to the dust deposition. Whether the mineralization of the upper lobes of lungs is dominated by calcium phosphates requires further investigation. We are not aware of a mineralogical study that would show the mineral composition of the apexes of lungs.

Age-related changes in lungs include, among others, progressive calcification of airways [53]. Based on the results of our study, it is tempting to hypothesize that the age-related lung calcification is not only caused by natural physiological processes but is also driven by the accumulation of exogenous particles. Perhaps, small (<3 cm in diameter) solid nodules commonly observed in the majority of elderly patients may have also developed on exogenous dust particles. Testing this hypothesis would require cross-sectional examination of the nodules.

Exogenous particle-induced calcification is not the only cell-mediated mineralization in the alveolar region of lungs. Long (>10 μm) and thin (<0.5 μm) asbestos fibers cannot be entirely internalized by alveolar macrophages and, in the process called "frustrated phagocytosis", are coated by a thin layer of Fe-containing proteins, goethite and apatite [40, 54]. However, our study shows that environmental exposure to mineral dust results principally in a large-scale particle-induced calcification of lungs. Precipitation of Mg-calcite and calcite on dust particles mask their occurrence in the lung. Thus, the actual number of inhaled dust particles deposited in lower lobes may be greater than observed because of the masking effect of carbonate coating.

6. Conclusions

While calcium salts precipitated in lungs are usually reported as phosphates (hydroxylapatite or whitlockite), calcium precipitates in RLL observed in this study are almost exclusively carbonates with Mg-calcite predominant in the submicron size range and calcite in larger grains and aggregates. Overall, Mg-calcite is the predominant carbonate in RLL with $MgCO_3$ content of <50 mol%. Thus, magnesium plays a significant role in lung mineralization, so far overlooked. The medical term "calcification" is somewhat misleading and does not reflect the actual chemical- and mineralogical compositions of lung endogenous mineralization. The calcium phosphate (hydroxyapatite) content in RLL is negligible. Lung fluids and blood plasma are saturated with respect to both apatite and calcite. Therefore, whether phosphate or carbonate will precipitate in the lungs depends on local conditions, namely CO_2 partial pressure. Elevated P_{CO2} in lower lobes favors precipitation of carbonates.

Precipitation of Mg-calcite and calcite is, at least in part, induced by the inhaled mineral dust particles settled in the alveolar sacs. Insoluble dust particles serve as nucleation sites for carbonate precipitates. The actual number of inhaled dust particles may be significantly larger than observed because of the masking effect of the carbonate coating. Our data support the observation of Churg and Wiggs [27] that total lower lobe particle retention appears to be independent of the amount of smoking.

Three possible pathways for carbonates precipitation on dust particles are inferred from this study: (1) Precipitation of ACC followed by its transformation to calcite; (2) precipitation of Mg-ACC

followed by its transformation to Mg-calcite; (3) precipitation of Mg-free ACC followed by Mg-calcite heterogeneous nucleation and crystal growth.

Author Contributions: Conceptualization, J.J.; methodology, M.J. and J.J.; validation, M.J., J.J., and B.S-K.; formal analysis, M.J. and J.J.; investigation, M.J. and B.S-K.; resources, J.J.; data curation, M.J.; writing—original draft preparation, J.J.; writing—review and editing, X.X.; visualization, M.J.; supervision, J.J. All authors have read and agreed to the published version of the manuscript.

Funding: This research received no external funding.

Acknowledgments: We are grateful to prof. Padhraig Kennan for improving the English of the manuscript. This work was financially supported by the statutory fund of the Institute of Earth Sciences, University of Silesia.

Conflicts of Interest: The authors declare no conflict of interest.

References

1. Bendayan, D.; Barziv, Y.; Kramer, M.R. Pulmanory calcification: a review. *Respir. Med.* **2000**, 94, 190-193.
2. Chan, E.D.; Morales, D.V.; Welsh, C.H.; McDermott, M.T.; Shwarz, M.I. Calcium deposition with or without bone formation in the lung. *Am. J. Respir. Crit. Care Med.* **2002**, 165, 1654–1669.
3. Farver, C.F. Other Nonneoplastic Focal Lesions, Inclusions, and Depositions. In: *Pulmonary Pathology*, 2nd ed.; Zander, D. S., Farver, C. F., Eds.; Elsevier, **2018**, pp. 514-533.
4. Belém, L.C.; Zanetti; G.; Souza Jr, A.S.; Hochhegger, B.; Giumães, M.D.; Nobre, L.F.; Rodrigues, R.S.; Marchiori, E. Metastatic pulmonary calcification: State-of-the-art review focused on imaging findings. *Respir. Med*. **2014**, 108, 668-676.
5. Khan, A.N.; Al-Jahdali, H.H.; Allen, C.M.; Irion, K.L.; Al Ghanem, S.; Koteyar, S.S. The calcified lung nodule: What does it mean? *Ann. Thorac Med*. **2010**, 5(2), 67-79.
6. Ferreira Francisco, F.A.; Pereira e Silva, J.L.; Hochhegger, B.; Zanetti, G.; Marchiori, E. Pulmonary alveolar microlithiasis. State-of-the-art review. *Respir Med*. **2013**, 107, 1-9.
7. Huang, Xi; Gordon, T.; Rom, W.N.; Finkelman, R.B. Interaction of iron and calcium minerals in coals and their role in coal-dust-induced health and environmental problems, In: *Medical mineralogy and geochemistry*; Sahai, N., Schoonen, A.A., Eds., Rev Mineral Geochem, **2006**, 64, 153-178.
8. Pope III, C. A.; Dockery, D. W. Health Effects of Fine Particulate Air Pollution: Lines that Connect. *J Air Waste Manag Assoc* **2006**, 56:6, 709-742.
9. Green, F.H.Y.; Vallyathan, V.; Hahn, F.F. Comparative pathology of environmental lung disease: An overview. *Toxicol. Pathol*. **2007**, 35, 136-147.
10. Naccache, J-M.; Monnet, I.; Nunes, H.; Billon-Galland, M-A.; Pairon, J-C.; Guillon, F.; Valeyre, D. Anthracofibrosis attributed to mixed mineral dust exposure: report of three cases, *Thorax* **2008**, 63, 655-657.
11. Kampa, M.; Castanas, E. Human health effects of air pollution. *Environ. Pollut.* **2008**, 151, 362-367.
12. Valavanidis, A.; Fiotakis, K.; Vlachogianni, T. Airborne particulate matter and human health: Toxicological assessment and importance of size and composition of particles for oxidative damage and carcinogenic mechanisms. *J. Environ. Sc. Health C* **2008**, 26, 339-362.
13. Hochgatterer, K.; Moshammer, H.; Haluza, D. Dust is in the air: Effects of occupational exposure to mineral dust on lung function in a 9-year study. *Lung* **2013**, 191, 257-263.
14. Camatini, M.; Gaultieri, M.; Sancini, G. Impact of the airborne particulate matter on the human health. In: *Atmospheric Aerosols: Life cycles and effects on air quality and climate*. Tomasi, C., Fuzzi, S., Kokhanovsky, A., Eds.; Wiley-VCH Verlag GmbH&Co. KGaA, Weinheim, Germany, **2017**, pp. 597-670, 2017.
15. Riediker, M.; Zink, D.; Kreylink, W.; Oberdörster, G.; Elder, A.; Graham, U.; Lynch, I.; Ichihara, G.; Kobayashi, T.; Hisanaga, N.; Umezawa, M.; Tsun-Jen Cheng; Handy, R.; Gulumian, M.; Tinkle, S.; Cassee, F. Particle toxicology and health. Where are we? *Part. Fiber Toxicol*. **2019**, 16(19). https://doi.org/10.1186/s12989-019-0302-8.
16. Brauer, M.; Avila-Casado, C.; Fortoul T.I.; Vedal, S.; Stevens, B.; Churg A. Air pollution and retained particles in the lung. *Environ. Health Perspect*. **2001**, 109, 1039-1043.
17. Hughes, L.S.; Cass, G.R.; Gone, J.; Ames, M.; Olmez, I. Physical and chemical characterization of atmospheric ultrafine particles in the Los Angeles area. *Environ. Sci. Technol*. **1998**, 32(9), 1153-1161.
18. Stettler, L.E.; Platek, S.F.; Riley, R.D.; Mastin, J.P.; Simon, S.D. Lung particulate burden of subjects from the Cincinnati, Ohio urban area. *Scanning Microsc*. **1991**, 5, 85-94.

19. Gibbs, A. R.; Pooley, F.D. Analysis and interpretation of inorganic mineral particles in "lung" tissues. *Thorax* **1996**, 51, 327-331.
20. Sellaro, R.; Sarver, E.; Baxter, D. A standard characterization methodology for respirable coal mine dust using SEM-EDX. *Resources* **2015**, 4, 939-957.
21. Churg, A.; Wiggs, B. Types, numbers, sizes, and distribution of mineral particles in the lungs of urban male cigarette smokers. *Environ Res*. **1987**, 42(1), 121-129.
22. Churg, A.; Wright, J.L.; Stevens, B. Exogenous mineral particles in the human bronchial mucosa and lung parenchyma. I. Nonsmokers in the general population. *Lung Res*. **1990**, 16(3), 159-175.
23. Paoletti, L.; Batisti, D.; Caiazza, S.; Petrelli, M.G.; Taggi, F.; De Zorzi, L.; Dinam A.; Donelli, G. Mineral particles in the lungs of subjects resident in the Rome area and not occupationally exposed to mineral dust, Environ. Res. **1987**, 44, 18-28.
24. Hunt, A.; Abraham, J.L.; Judson, B.; Berry, C.L. Toxicologic and epidemiologic clues from the characterization of the 1952 London smog fine particulate matter in archival autopsy lung tissues, Environ. Health Perspect. **2003**, 111 (9), 1209-1214.
25. Domingo-Neumann, R.; Southard, R.J.; Pinkerton, K.E. Mineral dust retained in lung tissue of residents reflects ambient PM10 mineralogy in Fresno, California. In: *Geological Society of America Abstracts with Programs* 41(7), p.90. **2009,** Portland, GSA Annual Meeting (18-21 October 2009).
26. Lowers, H.A.; Breit, G.N.; Strand, M.; Pillers, R. M.; Meeker, G. P.; Todorov, T. I.; Plumlee, G. S.; Wolf, R. E.; Robinson, M.; Parr, J.; Miller, R.; Groshong, S.; Green, F.; Rose C. Method to characterize inorganic particulates in lung tissue biopsies using field emission scanning electron microscopy, *Toxicol. Mech. Methods* **2018**, 28:7, 475-487, https://doi.org/10.1080/15376516.2018.1449042.
27. AAQR: Annual Air Quality Report for the Silesia voivodship in 2018. Main Inspectorate of Environmental Protection. Regional Department of the Environmental Monitoring in Katowice. April **2019**. Available online: www.katowice.wios.gov.pl/monitoring/informacje/stan2018/ocena_pow.pdf (accessed on 30 September 2020)
28. State of the Environment Report in the Voivodship of Silesia in 2018. Chief Inspectorate of the Environment Protection, Regional Inspectorate of the Environment Protection Katowice **2019**. Available online: www.katowice.wios.gov.pl/monitoring/raporty/2018/ocena2018.pdf (accessed on 30 May 2020).
29. Kowalska, M.; Skrzypek, M.; Kowalski, M.; Cyrys, J.; Niewiadomska, E.; Czech, E. The relationship between daily concentration of fine particulate matter in ambient air and exacerbation of respiratory diseases in Silesian Agglomeration, Poland. *Int. J. Environ. Res. Public Health* **2019**, 16, 1131; https://doi.org/10.3390/ijerph16071131.
30. Kowalska, M. Short-term effect of changes in fine particulate matter concentrations in ambient air to daily cardio-respiratory mortality in inhabitants of urban-industrial agglomeration (Katowice Agglomeration), Poland, In: *Air-quality – new perspective*. Intech Open, Lopez, G., Ed., **2012** 185-198, https://doi.org/10.5772/2561.
31. Kapka, L.; Zemła, B.F.; Kozłowska, A.; Olewińska, E.; Pawlas, N. Air quality vs. morbidity to lung cancer in selected provinces and localities of the Silesian region, (in Polish). *Przegl. Epidemiol*. **2009**, 63, 439-444.
32. Jabłońska, M.; Janeczek, J. Identification of industrial point sources of airborne dust particles in an urban environment by a combined mineralogical and meteorological analyses: A case study from the Upper Silesian conurbation, Poland. *Atmos. Pollut. Res*. **2019**, 10(3), 980-988.
33. Jabłońska, M. Mineral markers in lung tissues of individuals exposed to air pollution in the Katowice Conurbation (in Polish), Wydawnictwo Uniwersytetu Śląskiego, Katowice, **2013**.
34. Jablonska, M.; Janeczek, J.; Rietmeijer, F.J. Seasonal changes in the mineral compositions of tropospheric dust in the industrial region of Upper Silesia, Poland. *Mineral. Mag*. **2003**, 67 (6), 1231-1241.
35. Parkhurst, D.L. and Appelo, C.A.J.: Description of Input and Examples for PHREEQC Version 3—A Computer Program for Speciation, Batch-Reaction, One-Dimensional Transport, and Inverse Geochemical Calculations. US Geological Survey Techniques and Methods, Book 6, Chapter A43, 497 p., http://pubs.usgs.gov/tm/06/a43, 2013.
36. Möller, P; De Lucia, M. The impact of Mg^{2+} ions on equilibration of Mg-Ca carbonates in groundwater and brines. *Geochemistry* **2020**, 80(2), 125611.
37. Taunton, A.E.; Gunter, M.E.; Druschel, G.K.; Wood, S.A. Geochemistry in the lung: Reaction-path modeling and experimental examination of rock-forming minerals under physiologic conditions. *Am. Mineral*. **2010**, 95, 1624-1635.

38. Marques, M.R.C.; Loebeneberg, R.; Almukainzi, M. Simulated Biological Fluids with Possible Application in Dissolution Testing. Dissolution Technol. **2011**; https://dx.doi.org/10.14227/DT180311P15 (accessed 20.03.2020).
39. Utsonomiya, S.; Jensen, K.A.; Keeler, G.J.; Ewing, R.C. Uraninite and fullerene in atmospheric particulates, Environ. Sci. Technol. **2002**, 36(23), 4943-4947.
40. Di Giuseppe, D.; Zoboli, A.; Vigliaturo, R.; Gieré, R.; Bonasoni, M.P.; Sala, O.; Gualtieri, A.F. Mineral fibres and asbestos bodies in human lung tissue: A case study. *Minerals* **2019**, 9, 618; https://doi.org/10.3390/min9100618.
41. Lenders, J.J.M.; Dey, A.; Bomans, P.H.H.; Spielmann, J.; Hendrix, M.M.R.M.; de With, G.; Meldrum, F.C.; Harder, S.; Sommrdijk, N.A.J.M. High-magnesian calcite mesocrystals: A coordination chemistry approach. *J. Am. Chem. Soc*. **2012**, 134, 1367-1373.
42. Rodriguez-Blanco, J.D., Shaw, S., Benning, L.G. The kinetics and mechanisms of amorphous calcium carbonate (ACC) crystallization to calcite, via vaterite. *Nanoscale* **2011**, 3, 265-271.
43. Blue, C.R.; Giuffre, A.; Mergelsberg, S.; Han, N.; De Yoreo, J.J.; Dove, P.M. Chemical and physical controls on the transformation of amorphous calcium carbonate into crystalline $CaCO_3$ polymorphs. Geochim. Cosmochim. Acta **2017**, 196, 179-196.
44. Mayorga, I.C.; Astilleros, J.M.; Fernández-Días, L. Precipitation of $CaCO_3$ polymorphs from aqueous solutions: The role of pH and sulphate groups. *Minerals* **2019**, 9(178), https://doi.org/10.3390/min9030178.
45. Morse, J.W.; Arvidson, R.S.; Lüttge, A. Calcium carbonate formation and dissolution. *Chem. Rev*. **2007**, 107, 342-381.
46. Roggli, V.L.; Mastin, J.P.; Shellbourne, J.D.; Roe, M.; Brody, A.R. Inorganic particles in human lung: Relationship to the inflammatory response. In: *Inflammatory cells and lung disease*; Lynn, W.S., Ed.; Routledge Revivals., CRC Press, **2019**, Chapter 2.
47. Johnson, B.; Hochholzer, L. Pulmonary blue bodies. Hum. Pathol. **1981**, 12 (3), 258-266.
48. MacNee, W.; Donaldson, K. Mechanism of lung injury caused by PM10 and ultrafine particles with special reference to COPD. *Eur Respir J*. **2003**, 21. Suppl. 40, 47-51.
49. Scherbart, A.M.; Langer, J.; Bushmelev, A.; van Berlo, D.; Haberzettl, P.; van Schooten, F.J.; Schmidt, A.M.; Rose, C.R.; Schins, R.P.F., Albrecht, C. Contrasting macrophage activation by fine and ultrafine titanium dioxide particles is associated with different uptake mechanisms. Part. Fibre Toxicol. **2011**, 8, 31.
50. West, J.B. Regional differences in the lungs. *Postgrad. Med. J.* **1968**, 44(507), 120-122.
51. Klocke, R.A. Catalysis of CO_2 reactions by lung carbonic anhydrase. *J. Appl. Physiol*. **1978**, 44(6), 882-888.
52. Pan, H.; Darvell, B.W. Effect of carbonate on hydroxyapatite solubility. *Cryst. Growth Des*. **2010**, 10, 2, 845-850.
53. Gossner, J.; Nau, R. Geriatric Chest Imaging: When and how to image the elderly lung. Age-Related Changes, and Common Pathologies. Radiol. Res. Pract. **2013**, Article ID 584793, http://dx.doi.org/10.1155/2013/584793.
54. Bardelli, F.; Veronesi, G.; Capella, S.; Bellis, D.; Charles, L.; Cedola, A.; Belluso, E. New insights on the biomineralisation process developing in human lungs around inhaled asbestos fibres. Sci. Rep. **2017**, 7, 44862, https://doi.org/ 10.1038/srep44862.